Critical Observations for the Evaluation of Cement Hydration Models

Dale P. Bentz
Engineering Laboratory
National Institute of Standards and Technology
100 Bureau Drive Stop 8615
Gaithersburg, MD 20899-8615
E-mail: dale.bentz@nist.gov
Phone: (301)975-5865
Fax: (301)990-6891

Abstract

The development of computer models for cement hydration and microstructure development, with an explicit consideration of microstructure, has accelerated in the past 25 years, creating a need for a set of critical experimental observations that can be used in evaluating the model predictions. During this same time period, there have been rapid advances in experimental techniques for quantifying both the hydration rates and the produced microstructures. This paper utilizes several of these techniques to elaborate a preliminary set of experimental observations concerning the influence of water-to-cement ratio, cement particle size distribution, and curing conditions on hydration and microstructure development. Isothermal calorimetry provides a convenient measure of the ongoing hydration rates during the first 7 d of hydration, while low temperature calorimetry can be used to directly assess the percolation state of the capillary porosity and the quantity of freezable water in a hydrated cement paste. Conventional measurements of setting times, such as Vicat needle penetration, are related to the ongoing percolation transitions of the solids within the three-dimensional microstructure. Finally, since concretes in the field rarely experience saturated curing conditions, the influence of sealed curing on resultant degree of hydration and microstructure is examined. The presented data sets should provide a first step in performing a critical evaluation of existing and future computer models.

Keywords: Cement hydration; kinetics; microstructure; model; percolation; setting.

Introduction

Within the past 25 years, significant efforts have been devoted to advancing the computer modeling of cement hydration and microstructure development. At the present time, there are numerous models available for simulating various aspects of the complex reactions that occur and the microstructure that develops when cement is mixed with water [1-8]. These models differ in their fundamental approaches (particle-based models vs. pixel-based models), required inputs, and intended functions (generating microstructures, predicting properties, understanding hydration mechanisms). Rather than passing a value judgment on the appropriateness and value of one model vs. another, the purpose of this paper is to highlight several critical experimental observations that may prove useful in evaluating current and future models for hydration and microstructure development.

Any model is highly dependent on the quality and comprehensiveness of its inputs. For models of cement hydration and microstructure development, input typically consists of some computational representation of an arrangement of cement particles in water within a fixed volume. Diamond has pointed out some of the special considerations regarding the starting particles and their spatial arrangement for accurately modeling cement hydration [9]. A list of questions that could be posed concerning the starting cement paste microstructures and the model inputs would include:

- What range of particle sizes can be incorporated into the initial microstructure?
- What particle shapes can be incorporated into the initial microstructure?
- How can the cement clinker phases be distributed amongst the particles?
- Can the user specify the volume fractions of the cement clinker phases and various forms of gypsum?
- Can the phase surface area fractions be specified independently of the phase volume fractions?
- Can the particles be flocculated and/or dispersed spatially, to simulate the influence of a high range water-reducing agent for example?
- What other characteristics of the cement are required as inputs for the model (e.g., alkali content, free lime)?

This list is surely not exhaustive, but will serve as an adequate starting point for considering the comprehensiveness of a given model with respect to capturing the reality of the initial cement paste microstructure. The remainder of this paper will focus on expected outcomes of the models, consisting of a presentation of the experimental methods employed for obtaining the key observations, followed by a presentation and discussion of these critical observations themselves. These observations concern the influence of both water-to-cement ratio (*w/c*) and cement particle size distribution (PSD) on hydration kinetics and microstructure development and the effects of saturated vs. sealed curing conditions.

Experimental Methods

The experimental methods employed in this paper were chosen because of their wide availability and general usefulness for characterizing cement hydration reactions and their accompanying microstructural changes.

Isothermal Calorimetry – Hydration Kinetics

Isothermal calorimetry is rapidly becoming the experimental method of choice for evaluating early-age hydration kinetics, typically out to an age of 7 d to 14 d. In recent years, two ASTM standard test methods have been developed concerning this technique [10], ASTM C1702 describing the measurement of heat of hydration using isothermal conduction calorimetry and ASTM C1679 providing a standard practice for measuring hydration kinetics of hydraulic cementitious mixtures using isothermal calorimetry, as part of an evaluation of potential cement/admixture incompatibilities, for example. The basic procedure is to measure the heat generated by the hydration reactions for a specimen of cement paste or mortar that is maintained at isothermal conditions. Various commercial devices are now readily available for performing these measurements on cement-based and a wide variety of other materials. Generally, fresh

specimens are placed in a sealed vial before being introduced into the experimental apparatus, although many vendors do include options for in situ mixing of powders and liquids, typically using a small plastic paddle mixer within the specimen cell. A related experimental technique, semi-adiabatic calorimetry, in which the temperature of a fairly well-insulated hydrating specimen is monitored over time may provide experimental conditions more similar to field conditions of actual concrete structures and is currently being considered for standardization within ASTM [11].

Results of isothermal calorimetry typically consist of a data set providing the instantaneous heat release rate vs. time. These raw data can be integrated to obtain a curve of the cumulative heat release vs. time; normalization by the appropriate ultimate heat release value [12] can transform this integrated data into an estimate of the degree of hydration of the cement paste as a function of time. Mechanical and transport properties of a hardened cement paste are significantly influenced by its degree of hydration, so that computer models having an objective of predicting performance properties must provide an accurate portrayal of hydration kinetics, whether from first principle calculations, empirical relationships, or calibration vs. experimental data. In the present study, isothermal calorimetry will be employed to examine the influences of *w/c* and cement PSD on these hydration rates.

Vicat Needle Penetration – Percolation of Solids

While isothermal calorimetry monitors the rate of chemical reactions in a cementitious system, the actual hardening of the cement paste microstructure is a physical process that depends on building "bridges" between the reacting cement particles [12-17]. This percolation of a "solid" backbone across the 3-D volume of cement paste is typically assessed using a penetration test such as that described in the ASTM C 191 Standard Test Methods for Time of Setting of Hydraulic Cement by Vicat Needle [10]. While per the standard only the initial and final setting times are typically reported, the raw data includes measurements of the needle penetration throughout the setting/hydration process. The initial set time is selected as the time when a penetration of 25 mm is achieved, while the final set time occurs when no needle penetration is made into the now hardened specimen. In this study, graphs of the resistance to penetration in mm, calculated as (40 mm – the penetration depth), will be presented to highlight the influences of *w/c* and cement PSD on this solids percolation process. This setting process is a key concern of contractors and construction crews, as it dictates the timing of finishing and curing operations. Thus, the accurate prediction of setting times by a cement hydration and microstructure development model would increase its real world applicability. While this paper focuses on conventional Vicat needle evaluation of setting, ultrasonic measurements can also provide quantitative information on the percolation and mechanical property development of hydrating cement pastes [16,18].

Low Temperature Calorimetry – Percolation/Depercolation of Capillary Porosity

While setting is an example of a percolation process in hydrating cement pastes where the connectivity of the solid phases increases dramatically, there is an equally critical percolation process in which connectivity is gradually decreased and ultimately lost, namely the depercolation of the capillary porosity during hydration [19-21]. This depercolation results in a

significant reduction in transport rates within the material, particularly the permeability [19]. The determination of this depercolation point based on monitoring chemical shrinkage specimens of different thicknesses will be discussed subsequently. Another technique that can be used to determine the percolation state of the capillary porosity in a saturated specimen is low temperature calorimetry (LTC). Low temperature calorimetry measures the freezable water (pore solution) within a specimen of hardened cement paste as a function of temperature. The freezing temperature is controlled by the size of the pores in which freezing is occurring (among other variables such as pore solution ionic strength, etc.), so that a pore size distribution of a hardened cement paste specimen can be determined via thermoporometry without any drying of the specimen [22]. A freezing scan can also be used to assess the percolation state of the capillary porosity, as in general, water in a larger pore will only freeze when a previously formed freezing front penetrates the smaller pore entryways. Thus, during an initial freezing scan, the presence or absence of a peak at a temperature in the range of -15 °C to -20 °C is indicative of the percolation/depercolation state of the capillary porosity in the specimen [21,23].

Chemical Shrinkage – Hydration Kinetics and Depercolation of Capillary Porosity

Measurements of chemical shrinkage can serve a dual role of assessing hydration kinetics (as with isothermal calorimetry) and the depercolation transition (as with LTC). Because the hydration products occupy less volume than the reactants, there is a net chemical shrinkage during hydration that will result in a measurable imbibition of water by a hydrating cement paste specimen [24]. This technique has been standardized as the ASTM C1608 Standard Test Method for Chemical Shrinkage of Hydraulic Cement Paste [10], where a specimen thickness of 5 mm to 10 mm is recommended. The standard describes both gravimetric and volumetric methods for measuring the amount of water imbibed as a function of time. The agreement between degree of hydration as determined via isothermal calorimetry vs. that determined via chemical shrinkage is usually quite reasonable [25] and recently, an isothermal calorimeter has been modified to provide both measurements simultaneously [26].

If results for cumulative chemical shrinkage per gram of cement are plotted as a function of specimen thickness, initially the various curves will overlap, but once depercolation of the capillary porosity occurs, the thicker specimens (> 10 mm for example) will indicate less chemical shrinkage than the thinner ones as the depercolation of the capillary porosity will reduce the water imbibition rate to a value below that required to maintain saturated conditions at the current hydration rate, leading to self-desiccation within a portion of the thicker specimen [27]. Recently, it has been demonstrated that these chemical shrinkage depercolation measures correspond well with the values determined using the LTC technique for ordinary portland cement pastes [28].

Scanning Electron Microscopy and Three-Dimensional Microtomography – Observation of Microstructure

When evaluating a computer model vs. its real world counterpart, human perception will always play a critical role. For this reason, obtaining two or three-dimensional images of the real microstructures is invaluable for comparing to the microstructures that are output by the computer models. While scanning electron microscopy (SEM) can provide high resolution two-

dimensional images of real microstructures, meticulous specimen preparation (polishing, etc.) is required and tens of images must be acquired to provide a truly representative view of the microstructure. Conversely, X-ray microtomography offers the possibility to capture three-dimensional microstructures in situ, throughout the hydration process (or at least after setting has occurred). For example, a series of hydrating cement pastes have been successfully imaged using the European Synchrotron Radiation Facility; this Visible Cement Data Set is available for downloading at http://visiblecement.nist.gov [29]. For most tomography systems, there is sufficient phase contrast to isolate unhydrated cement, hydration products, and porosity [29]; SEM may provide sufficient contrast to further isolate calcium hydroxide from the other hydration products. The spatial resolution of the readily available X-ray microtomography systems is generally on the order of one micrometer, although some specialized facilities and newer models are providing sub-micrometer resolution. Here, these techniques will be employed to examine the influence of saturated vs. sealed curing conditions on microstructural development during hydration.

Critical Observations

Influence of Water-to-Cement Ratio (w/c)

Since the earliest days of concrete technology, the relationship between *w/c* and compressive strength has been well documented [30,31]. For conventional concretes, a reduction in *w/c* leads to higher compressive strengths, through its concurrent reduction in capillary porosity and/or pore sizes. Since compressive strength development is dependent on hydration rates, it is surprising that the effect of *w/c* on early age hydration rates is not as dramatic [32,33]. This is clearly illustrated by the isothermal calorimetry results presented in Figure 1 for cement pastes with *w/c* between 0.325 and 0.425, a range that encompasses many of the mixtures commonly employed in concrete construction. In the top portion of Figure 1, it can be observed that the heat release rates for the four cement pastes are basically identical out to an age of 24 h; similar results have been obtained by Sandberg and Roberts [33] for cement pastes with *w/c* between 0.35 and 0.45. At later ages, the cumulative heat release curves diverge, as shown in the bottom graph of Figure 1. Space limitations and self-desiccation (as the isothermal calorimetry specimens are hydrating under sealed conditions) began to limit the hydration rates of the specimens with the lower *w/c*, while the higher *w/c* ones continue to hydrate at a more rapid rate. It should be noted that these results were obtained on cement pastes and could be different in mortars or concretes, due to differences in mixing energy, etc. [32].

Deviations from this conventional behavior would also be expected for cement pastes prepared with either an extremely low or extremely high *w/c*. It is often difficult to prepare and evaluate cement pastes with *w/c* of 0.45 and higher due to segregation and bleeding effects. For lower *w/c* ratios, assuring adequate mixing and avoiding excessive temperature rises during mixing become experimental concerns. Still, as the *w/c* approaches 0, the hydration rates would also be expected to approach 0. The results in Figure 1 do demonstrate, though, that for a wide range of *w/c* that encompasses many mixtures of practical interest, early-age (< 24 h) hydration rates are independent of *w/c*, while at later ages, rates are higher for higher *w/c* mixtures. It is at least this behavior that should be accurately reproduced by a hydration and microstructure development model of cement paste.
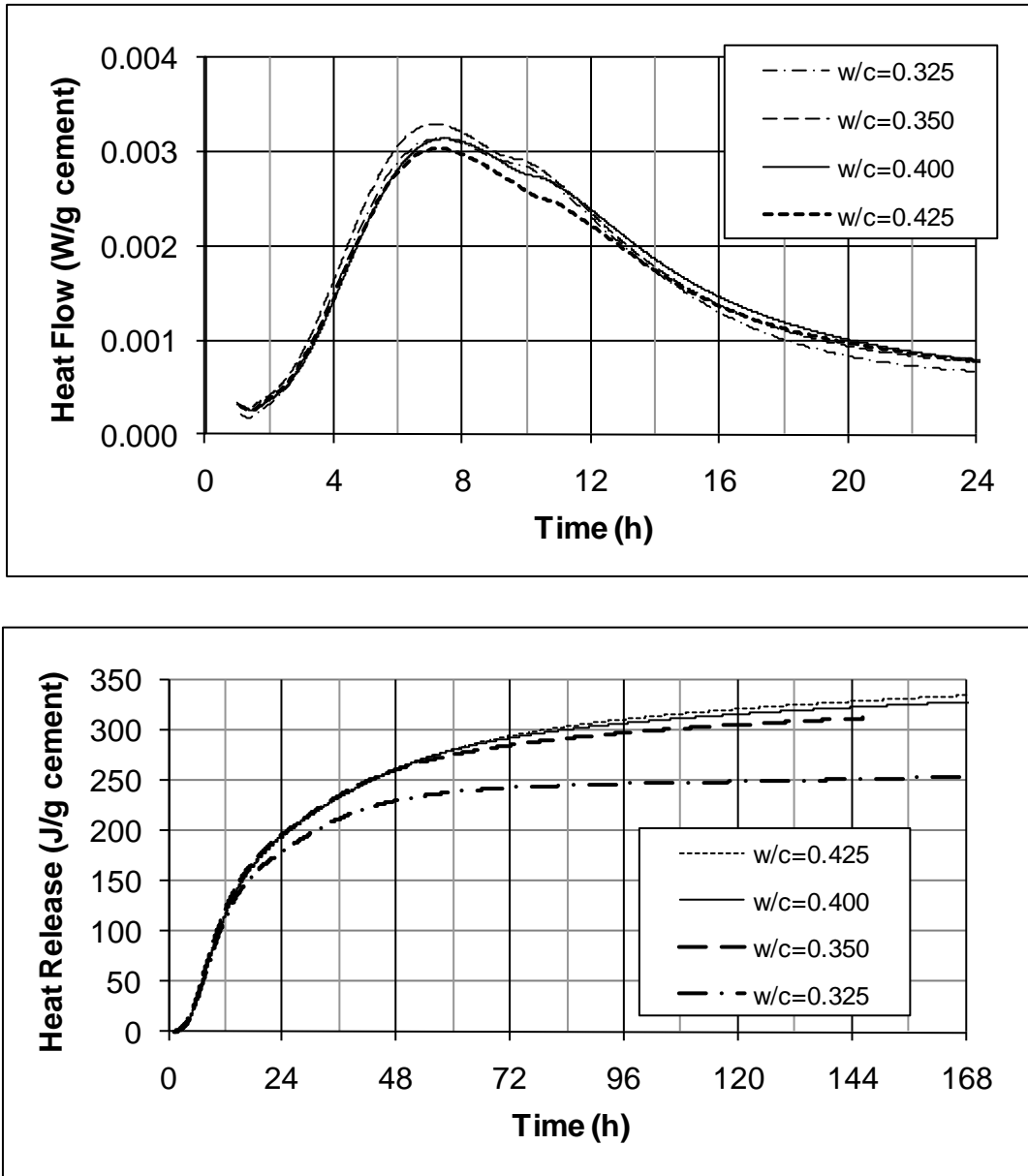
Fig. 1 Isothermal calorimetry results for heat release rate (top) and cumulative heat release (bottom) per gram of cement vs. curing time for four different *w/c* pastes prepared from a single cement [32]

Because setting is a physical process that is dependent on both hydration rates and the spacing between cement particles [14], setting times, unlike early-age hydration rates, are strongly dependent on *w/c*. This is illustrated definitively in Figure 2 that shows both experimental and computer modeling results exemplifying the influence of *w/c* on measured Vicat needle resistance and modeled solids percolation, for *w/c* ranging from 0.3 to 0.45. As would be expected, the lower *w/c* mixtures require less time to achieve percolation (set), due to their reduced initial particle spacing [34]. Several recent studies have demonstrated correlation between experimental measurements of setting, such as ultrasonics and needle penetration, and various model-based measurements of solids percolation [13,14,16,17]. Thus, it is important for

cement hydration and microstructural models first to provide a measure of solids percolation and then to duplicate these commonly observed influences of *w/c* on setting.
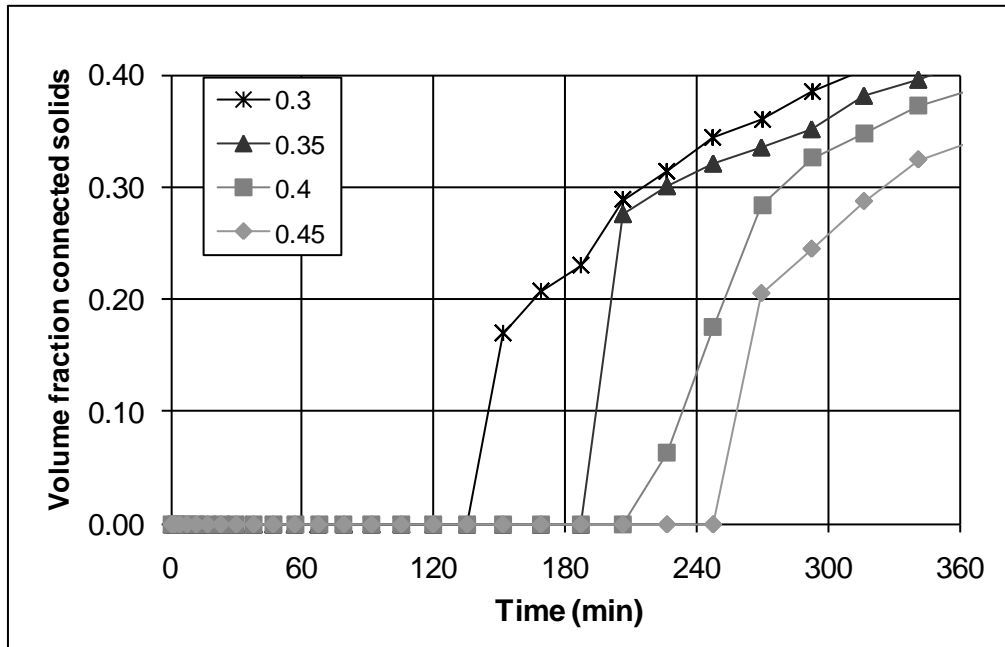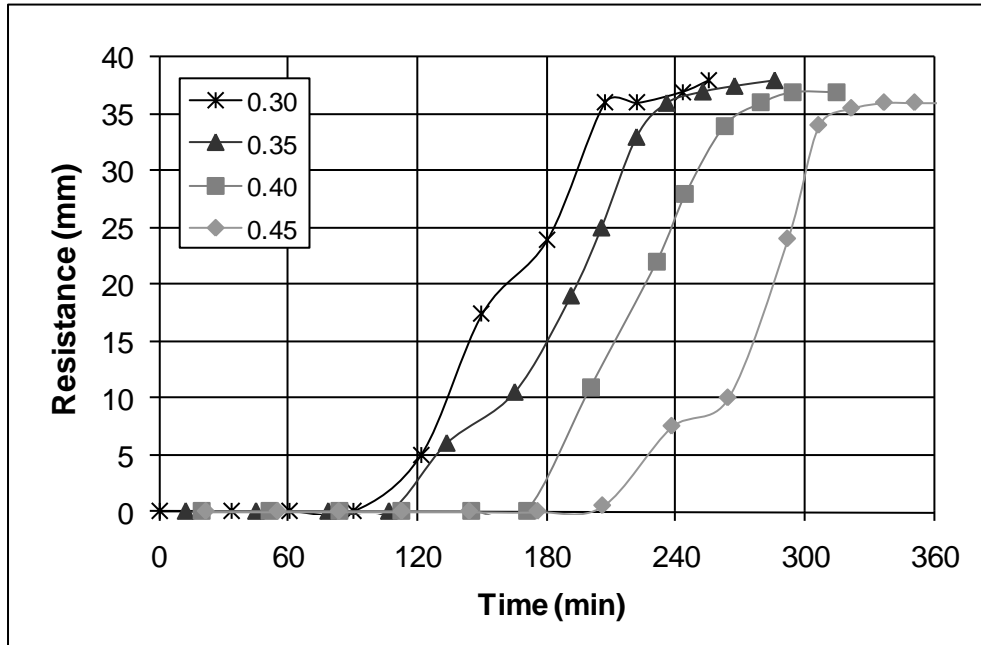

Fig. 2 Vicat needle resistance measurement (top) and computer model (CEMHYD3D) percolation predictions (bottom) for cement pastes prepared from a single cement at four different *w/c* [14]

Influence of Cement Particle Size Distribution (PSD)

Cement particle size distribution influences a wide range of early-age properties [25,35], as it controls the surface area of cement available for reaction with water and influences the spacing between particles [34]. One would expect finer cements to react faster and in general, this is indeed the case. However, in terms of the length of the induction period and the timing of the peak hydration rate, the effects of cement PSD are much less pronounced. This is illustrated by the two sets of isothermal calorimetry results provided in Figures 3 and 4. Results in Figure 3 are for three different cements produced from the same clinker [35], but ground to different finenesses with each individually optimized for sulfate content by the manufacturer, as finer cements may require a higher sulfate content. For the results in Figure 4, a commercial cement was first classified to have four different D90 values (fine to coarse ranging from 7.5 µm to 20 µm), and the remainder of the cement then reground to match that same D90. Effectively, these four cements have different finenesses, but the same overall calcium sulfate content. These four cements were then employed in producing blended cements with various replacement levels of a Class F fly ash for cement. The Class F fly ash employed was rather coarse and did not contribute significantly to the reactions during the first 16 h, and thus the results in Figure 4 are normalized with respect to mass of cement. In this case, the four heat release rate curves overlap one another between 3 h and 4 h.
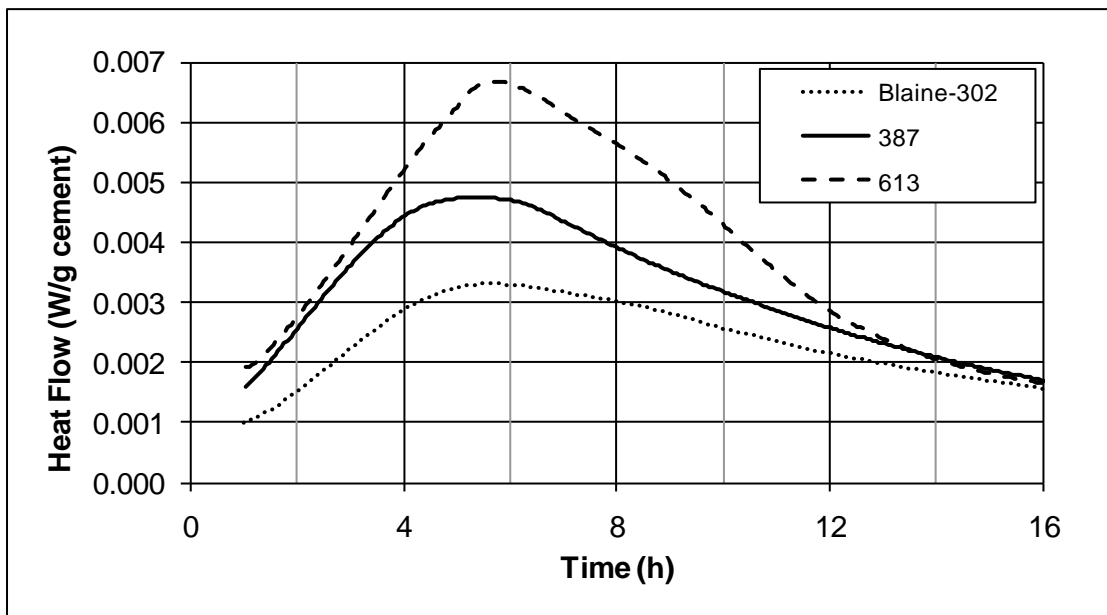

Fig. 3 Measured heat release rates vs. time for *w/c*=0.4 cement pastes prepared from cements of three different finenesses, but with the same clinker source (adapted from ref. 35). Blaine finenesses listed in the legend are in units of m^2/kg

The fact that the times for the end of the induction period and the times of maximum heat release rate are not strongly dependent on cement PSD (and thus exposed surface area) suggests that not only are the particles hydrating independently during these first few hours of curing, but also that these times are likely controlled by the formation of some type of surface layer on the cement particle surfaces, perhaps achieving a critical thickness [3]. This independence of these

times with respect to cement PSD is thus another critical experimental observation that ideally should be reproduced by a cement hydration and microstructure development model.
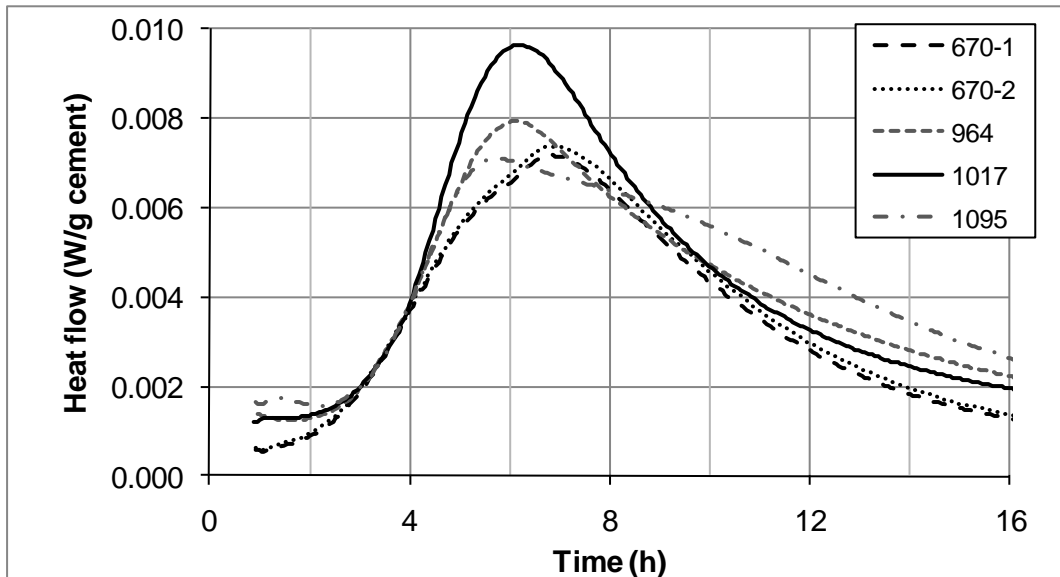

Fig. 4 Measured heat release rates vs. time for blended cement pastes with 35 % Class F fly ash by volume and a constant volume fraction of water of 0.528, prepared from cements of four different finenesses, but with the same clinker source. Fineness of the cement in m^2/kg as measured by the surface area determined from PSD measurements is indicated in the legend. Two sets of results are shown for the coarsest cement to provide some indication of measurement variability

As with the influences of *w/c*, setting times are also highly dependent on cement fineness. This is illustrated in Figure 5 that shows the Vicat needle resistance measurements for the three cements prepared from the same clinker, but ground to different finenesses. The isothermal calorimetry results given above indicate that once the induction period is past, the finer cements do hydrate at a higher rate (per unit mass of cement), which should reduce the setting time. However, a finer cement typically contains more cement particles per unit volume so that more hydration product "bridges" connecting particles must be built than in the case of a coarser cement [14, 36], which could increase the setting time, particularly when the particles are highly flocculated in the absence of a water reducer. In practice, the former effect normally dominates over the latter one, so that initial and final setting times can be reduced by several hours as cement fineness progresses from a coarse Type I/II cement to a typical Type III cement. The ability of a cement hydration and microstructure development model to capture these effects would be beneficial to those wanting to predict field performance with respect to setting and finishing for particular materials of interest.

Depercolation of Capillary Porosity

While the total solids are percolating across the microstructure to rigidify and strengthen the cement paste, the capillary porosity is undergoing an equally important depercolation transition. The initial 3-D capillary porosity, composed of the water-filled spaces between the
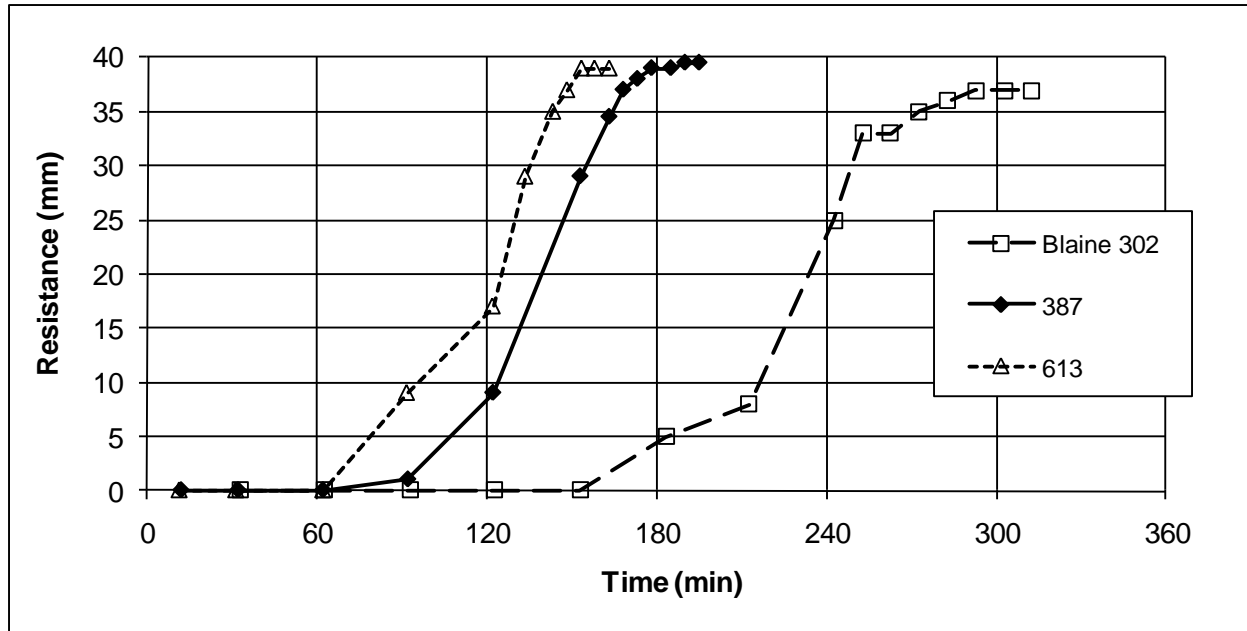
Fig. 5 Measured Vicat needle resistance vs. time for *w/c*=0.4 cement pastes prepared from cements of three different finenesses (in m²/kg), but with the same clinker source (adapted from ref. 35)

cement particles, is highly percolated, but during hydration it may become depercolated, depending on the initial *w/c*, amongst other variables. This depercolation was first identified by Powers, Copeland, and Mann [19] and is important from a practical viewpoint for several reasons. First, once capillary depercolation occurs, the penetration of externally-supplied water for curing will become severely limited, hence, the advent of internal curing as a method to distribute this needed additional water uniformly throughout the microstructure [37]. Second, a depercolated capillary pore structure will greatly reduce the transport coefficients of the material, relative to one in which these larger pores remain percolated. In fact, it was via the measurement of permeability that Powers et al. inferred that this depercolation process was in fact occurring [19].

Low temperature calorimetry provides a convenient means for directly assessing the volume of water-filled percolated capillary pores within a hydrated cement paste. During a freezing scan, the presence/absence of a peak in the range of -15 °C to -20 °C indicates the percolation/depercolation state of the capillary pores [23], while the size of the peak (or more accurately the area beneath it) indicates the volume of freezable water or percolated capillary pore space [21]. Figure 6 illustrates experimental measurements of this freezable water volume as compared to predictions from one of the commonly available hydration models, with reasonable agreement between the two. While numerous experimental [19,21,27,28] and some computer modeling results [20,21] have indicated that this capillary porosity depercolation occurs at about 20 % capillary porosity, independent of *w/c*, other models have suggested a much lower depercolation threshold in the range of 3 % to 5 % [38,39]. Obviously, the ability of a hydration and microstructure model to accurately represent this depercolation process will be critical to its success in predicting curing requirements and transport properties.
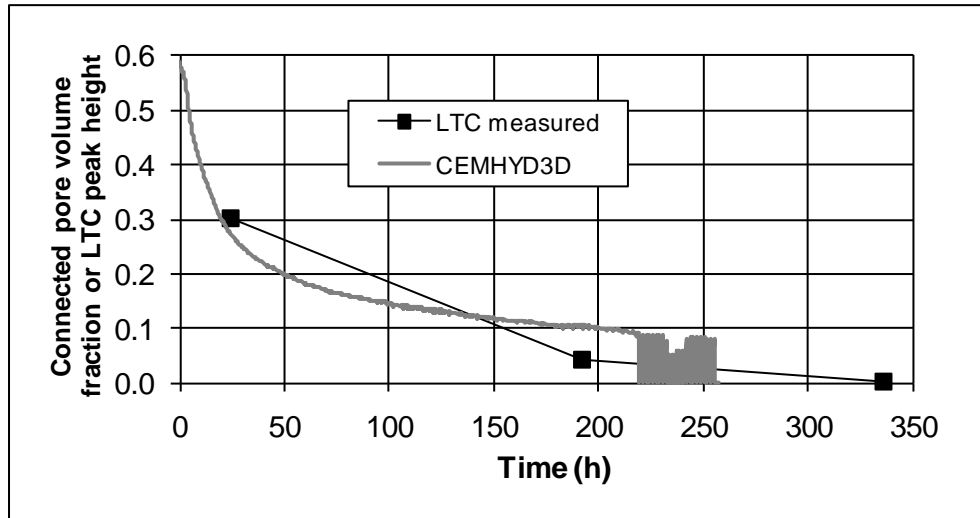
Fig 6 Comparison of LTC estimated and CEMHYD3D modeled percolated capillary porosity fractions vs. time for *w/c*=0.45 cement paste hydrated under saturated conditions as 40 °C [21]

Influence of Curing Conditions (Saturated vs. Sealed Curing)

Most field concretes do not maintain saturated conditions throughout the time period of cement hydration. Typically, partially saturated conditions will be produced due to self-desiccation accompanying the chemical shrinkage that is characteristic of the hydration reactions and/or further removal of water due to drying/evaporation. Hydration rates and the developed microstructure are strongly dependent on moisture availability and will differ significantly for hydration under saturated vs. sealed conditions, for example [40]. Figures 7 and 8 illustrate these effects, showing the dependence of both hydration rates and long term microstructure on curing conditions. In Figure 7, hydration rates were assessed using loss-on-ignition measurements of non-evaporable water content. For these *w/c*=0.35 cement pastes, a significant difference in achieved hydration is observed for ages of 7 d and beyond. These effects would be even more pronounced for lower *w/c* cement pastes where chemical shrinkage would produce an even more rapid decrease in internal relative humidity and hydration rates. In addition to the influence on intermediate age hydration rates, curing conditions also dramatically alter the developed microstructure as exemplified by the micrographs in Figure 8 for a *w/c*=0.3 cement paste cured for 94 d. The specimen cured under sealed conditions contains more and larger unhydrated cement particles and more and larger (empty) capillary pores. These microstructural differences would influence both mechanical and transport properties and, therefore, the ability of a cement hydration and microstructure development model to handle a wide variety of curing conditions is a definite advantage. For example, when modeling autogenous shrinkage, modeling hydration under sealed conditions is a necessity [41]. As resultant microstructures are also dependent on curing temperature [42], models that reliably operate at different temperatures, or under adiabatic, semi-adiabatic, and isothermal conditions are further preferred.
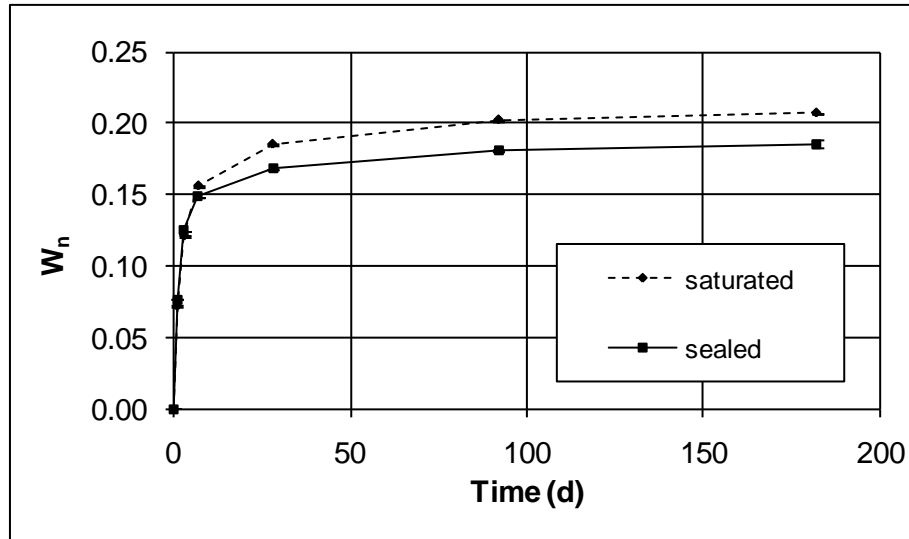
Fig. 7 Measured non-evaporable water content vs. time for *w/c*=0.35 cement pastes hydrated under saturated and sealed curing conditions (adapted from ref. 40). Vertical error bars indicate +/- one standard deviation for experimental measurements and generally fall within the size of the symbol plotted

Summary and Prospectus

There now exists a set of mostly standardized experimental techniques that are invaluable for quantifying the hydration rates and examining the microstructure development of hydrating cement pastes. While more elaborate techniques (such as neutron scattering, neutron magnetic resonance, and X-ray diffraction to name a few) can provide more detailed information on the ongoing hydration process with respect to individual or multiple phases, those techniques described herein should be readily available to a majority of researchers in this field. Simply examining the influence of basic variables like *w/c* and cement PSD on hydration kinetics and resultant microstructures provides a valuable data set, as illustrated herein, for better understanding the hydration process and for better evaluating existing and future computer models with respect to their representation of reality. As advances continue to be made for both the experimental and modeling approaches, their integration will surely lead to a more complete understanding of the cement hydration process. This in turn will allow for better control of this process in order to engineer the performance properties and sustainability of this critical infrastructure material.
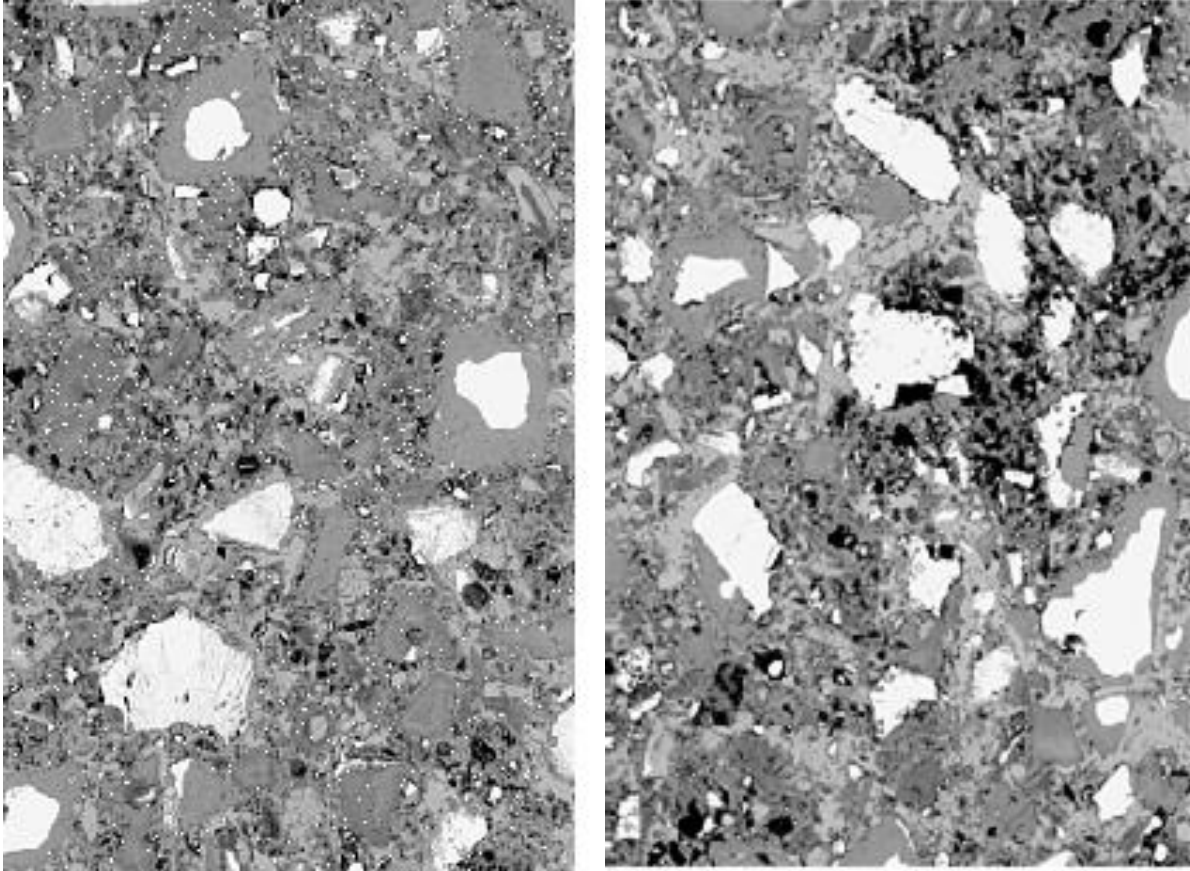
Acknowledgements

Fig. 8 Backscattered electron images (128 µm x 190 µm) of cement pastes hydrated for 94 d under saturated (left) and sealed (right) conditions, w/c=0.3. Unhydrated cement is white, porosity is black, calcium hydroxide is light grey, and calcium silicate hydrate gel and other hydration products are dark grey

References

1) Bentz, D.P.: CEMHYD3D: A three-dimensional cement hydration and microstructure development modeling package. Version 3.0. NISTIR **7232**, U.S. Department of Commerce, June (2005)

2) Bishnoi, S., Scrivener, K.L.: µic: A new platform for modelling the hydration of cement. Cem. Concr. Res. 39 (4), 266-274 (2009)

3) Bullard, J.W.: A determination of hydration mechanisms for tricalcium silicate using a kinetic cellular automaton model, J. Amer. Ceram. Soc. 91 (7), 2088-2097 (2008)

4) Bullard, J.W., Enjolras, E., George, W.L., Satterfield, S.G., Terrill, J.E.: A parallel reaction-transport model applied to cement hydration and microstructure development. Modelling Simul. Mater. Sci. Eng. (2010) doi: 10.1008/0965-0393/18/2/025007

5) Chen, W.: Hydration of slag cement – Theory, modeling, and application. Ph.D. Thesis, University of Twente, The Netherlands (2006) 223 p.

6) Maekawa, K., Chaube, R., Kishi, T.: Modelling of Concrete Performance: Hydration, Microstructure Formation and Mass Transport. E&FN Spon, London, (1999)

7) Van Breugel, K.: Simulation of hydration and formation of structure in hardening cement-based materials. Ph.D. Thesis, Delft University, The Netherlands (1991) 295 p.

8) Van Eijk, R.: Hydration of cement mixtures containing contaminants. Ph.D. Thesis, University of Twente, The Netherlands (2001) 200 p.

9) Diamond, S.: An "Unmodel" of portland cement hydration. 2nd Intl. Conf. Advances in Concrete Through Science and Engineering, Quebec, Sept. (2006)

10) ASTM International, ASTM Standards on Disc, Volume 04.01 Cement; Lime; Gypsum, ASTM International (2007)

11) Cost, V.T., Gardiner, A.: Practical concrete mixture evaluation via semi-adiabatic calorimetry. NRMCA Technology Forum, 21 pp. (2009)

12) Bentz, D.P.: Verification, validation, and variability of virtual standards. in Proceedings of the 12th International Congress on the Chemistry of Cement, Montreal (2007)

13) Princigallo, A., Lura, P., van Breugel, K., Levita, G.: Early development of properties in a cement paste: A numerical and experimental study. Cem. Concr. Res. 33, 1013-1020 (2003)

14) Bentz, D.P.: Cement hydration: Building bridges and dams at the microstructure level. Mater. Struct. 40 (4), 397-404 (2007)

15) Sant, G., Ferraris, C.F., Weiss, J.: Rheological properties of cement pastes: A discussion of structure formation and mechanical property development. Cem. Concr. Res. 38 (11), 1286-1296 (2008)

16) Robeyst, N.: Monitoring setting and microstructure development in fresh concrete with the ultrasonic through-transmission method. Ph.D. Thesis, Ghent University, Belgium (2009) 251 p.

17) Stefan, L., Benboudjema, F., Torrenti, J.-M., Bissonnette, B.: Prediction of elastic properties of cement pastes at early ages. Computational Mater. Sci. 47, 775-784 (2010)

18) Sayers, C.M., Grenfell, R.L.: Ultrasonic propagation through hydrating cements. Ultrasonics 31, 147-153 (1993)

19) Powers, T.C., Copeland, L.E., Mann, H.M.: Capillary continuity or discontinuity in cement paste. PCA Bulletin 10, 2-12 (1959)

20) Bentz, D.P., Garboczi, E.J.: Percolation of phases in a three-dimensional cement paste microstructural model. Cem. Concr. Res. 21, 324-344 (1991)

21) Bentz, D.P.: Capillary porosity depercolation/repercolation in hydrating cement pastes via low temperature calorimetry measurements and CEMHYD3D modeling. J. Amer. Ceram. Soc. 89 (8), 2606-2611 (2006)

22) Sun, Z., Scherer, G.W.: Pore size and shape in mortar by thermoporometry. Cem. Concr. Res. 40 (5), 740-751 (2010)

23) Snyder, K.A., Bentz, D.P.: Suspended hydration and loss of freezable water in cement pastes exposed to 90 % relative humidity. Cem. Concr. Res. 34 (11), 2045-2056 (2004)

24) Bentz, D.P.: Three-dimensional computer simulation of cement hydration and microstructure development. J. Amer. Ceram. Soc. 80 (1), 3-21 (1997)

25) Bentz, D.P., Sant, G., Weiss, W.J.: Early-age properties of cement-based materials: I. Influence of cement fineness. ASCE J. Mater. Civ. Eng. 20 (7), 502-508 (2008)

26) Lura, P., Winnefeld, F., Klemm, S.: A method for simultaneous measurements of heat of hydration and chemical shrinkage of hardening cement pastes. J. Thermal Analysis Calorimetry (2010) doi:10.1007/s10973-009-0586-2

27) Geiker, M.R.: Studies of portland cement hydration: Measurements of chemical shrinkage and a systematic evaluation of hydration curves by means of the dispersion model. Ph.D. Thesis, Technical University of Denmark, Lyngby, Denmark (1983)

28) Sant, G.: Fundamental investigations related to the mitigation of volume changes in cement-based materials at early ages. Ph.D. Thesis, Purdue University, West Lafayette, IN (2009)

29) Bentz, D.P., Mizell, S., Satterfield, S., Devaney, J., George, W., Ketcham, P., Graham, J., Porterfield, J., Quenard, D., Vallee, F., Sallee, H., Boller, E., Baruchel, J.: The visible cement data set. NIST J. Res. 107 (2), 137-148 (2002)

30) Féret, R. : Etudes sur la constitution intime des mortiers hydrauliques. Bulletin de la Société d'Encouragement pour Industrie Nationale, 5th series, 2, 1591-1625 (1897)

31) Abrams, D.: Design of concrete mixtures. Structural Materials Research Laboratory, Bulletin No. 1, PCA LS001 (1918) also available at: http://www.cement.org/pdf_files/LS001.pdf.

32) Bentz, D.P., Peltz, M.A., Winpigler, J.: Early-age properties of cement-based materials: II. Influence of water-to-cement ratio. ASCE J. Mater. Civ. Eng. 21 (9), 512-517 (2009)

33) Sandberg, P.J., Roberts, L.R.: Cement-admixture interactions related to aluminate control. J. ASTM Inter. 2 (6), 1-14 (2005)

34) Bentz, D.P., Aitcin, P.C.: The hidden meaning of water-to-cement ratio. Concr. Inter. 30 (5), 51-54 (2008)

35) Bentz, D.P.: Blending different fineness cements to engineer the properties of cement-based materials. Mag. Concr. Res. 62 (5), 327-338 (2010)

36) Bentz, D.P., Garboczi, E.J., Haecker, C.J., Jensen, O.M.: Effects of cement particle size distribution on performance properties of cement-based materials. Cem. Concr. Res.. 29 (10), 1663-1671 (1999)

37) Bentz, D.P., Lura, P., Roberts, J.W.: Mixture proportioning for internal curing. Concr. Inter. 27 (2), 35-40 (2005)

38) Ye, G., Van Breugel, K., Fraaij, A. L. A.: Three-dimensional microstructure analysis of numerically simulated cementitious materials. Cem. Concr. Res. 33, 215–222 (2003)

39) Ye, G.: Percolation of capillary pores in hardening cement pastes. Cem. Concr. Res. 35, 167-176 (2005)

40) Bentz, D.P., Stutzman, P.E.: Curing, hydration, and microstructure of cement paste. ACI Mater. J. 103 (5), 348-356 (2006)

41) Rajayogan, V.: Autogenous shrinkage in cementitious systems. Ph.D. Thesis, The University of New South Wales, Australia (2009) 390 p.

42) Kjellsen, K.O., Detwiler, R.J., Gjorv, O.E.: Backscattered electron imaging of cement pastes hydrated at different temperatures. Cem. Concr. Res. 20, 308-311 (1990)